AI-based Pilotless Communication: Experimental Validation via Channel Emulation and Indoor Over-the-air Testing

Kyungpil Lee [1], Sangmin Jung [1], Giwan Choi [1], Dongwook Kim [1], Takki Yu [1], Dani Korpi [2], Jaime J. L. Quispe [3], Hiroto Yamamoto [4], Daisei Uchida [4], Huiling Jiang [5], Satoshi Suyama [5]

[1] Infra Tech. Office, SK Telecom Co., Ltd., Seoul, South Korea, Email: {kyungpil.lee, tojsm, giwan.choi, kimdw, takki.yu}@ sk.com
[2] Radio Systems Research, Nokia Bell Labs, Espoo, Finland, Email: dani.korpi @ nokia-bell-labs.com
[3] Platforms & ASIC Research, Nokia Bell Labs, Stuttgart, Germany, Email: jaime.luque_quispe @ nokia-bell-labs.com
[4] Access Network Service Systems Laboratories, NTT, Inc., Kanagawa, Japan, Email: {hiroto.yamamoto, daisei.uchida}@ ntt.com
[5] 6G-Tech Department, NTT DOCOMO, INC., Kanagawa, Japan, Email: {jiang, satoshi.suyama.zd}@ nttdocomo.com

***Abstract*—AI technologies are expected to be fully integrated into mobile communication systems in the 6G era, especially bringing significant advances in the Radio Access Network (RAN) domain. In particular, extensive research has been conducted to apply AI to the air interface in order to enhance the performance of mobile communication, and AI-based pilotless communication has been proposed as a promising use case. In this paper, a proof-of-concept (PoC) system for AI-based pilotless communication is developed, and experimental results via channel emulation and over-the-air (OTA) testing in practical indoor environments are presented. In all tested conditions and environments, the proposed method was observed to improve throughput performance. Furthermore, the channel emulator-based test results show that the proposed method can maintain robustness even under channel conditions not considered during training and can be more effective in rapidly varying channel conditions. The proposed method improves throughput performance by 13–18% in the practical indoor environments.**

Keywords— 6G, artificial intelligence, AI-native air interface, convolutional neural network, pilotless communication, throughput, channel emulation, indoor over-the-air testing

I. Introduction

While large language models (LLMs) have fueled advances in generative AI, there is now a growing shift toward physical AI, which aims to solve real-world problems and support decision-making in many industries [1]. This shift signifies not only advances in language understanding, but also a broader transformation in how AI technologies are shaping and optimizing industrial processes, infrastructure, and services. In the mobile communication industry, it is expected that AI technologies will be fully integrated into mobile communication systems in the 6G era [2], thereby driving considerable advancements particularly in the Radio Access Network (RAN) domain, which accounts for the majority of mobile network infrastructure investments [3, 4].

Especially, a concept called AI-native air interface has been proposed [5] and many studies have been conducted to apply AI to the air interface in order to improve the performance of the mobile network. In 3GPP, the use cases of channel state information (CSI) feedback enhancement, beam management, and positioning accuracy enhancement were discussed in Release 19 [6]. In addition, an AI-based orthogonal frequency-division multiplexing (OFDM) receiver to handle waveforms distorted by power amplifier non-linearity was proposed in [7], and an AI-based beamforming method was proposed in [8] to predict downlink channel states from uplink estimates, thereby enhancing beamforming performance. Furthermore, [9] proposed another AI-based OFDM receiver which can reduce the number of pilot symbols, and an AI-based pilotless communication method was proposed in [10] as an extension of [9].

In this paper, we develop a proof-of-concept (PoC) system for [10] and present experimental results obtained through channel emulation and over-the-air (OTA) testing in practical indoor environments. The results demonstrate that the proposed method enhances throughput performance by more than 13% across all tested conditions and environments, and is shown to be more effective under rapidly varying channel conditions.

II. AI-based Pilotless Communication

Fig. 1 shows the overall block diagram of the AI-based pilotless communication system. In the transmitter, AI is applied to the modulation processing; the data is modulated using an irregular learned constellation vector, jointly pre-trained with the receiver output [10]. On the receiver side, the conventional channel estimation, equalization, and symbol de-mapping processes are replaced by an AI model based on a residual network (ResNet)-type convolutional neural network (CNN) [9]. ResNets have previously been employed for image segmentation tasks, where the neural network is required to classify each pixel in an image. This approach is analogous to OFDM reception, in which the receiver must classify each resource element according to the symbol it represents. In this context, a two-dimensional resource grid spanning the

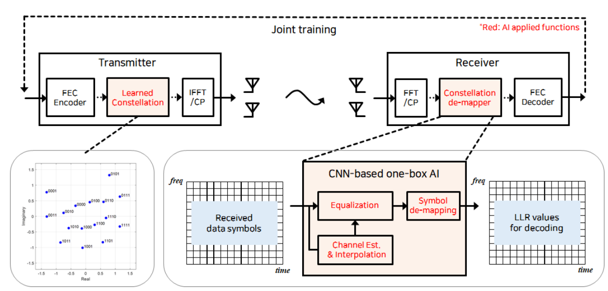

Fig. 1. Block diagram of AI-based pilotless communication system

frequency and time axes can be interpreted as the image. The AI model in the receiver processes the frequency-domain data obtained by applying the Fourier transform to the received signal and outputs the bit-level log-likelihood ratio (LLR) values. The AI models at the transmitter and receiver are jointly trained in an end-to-end manner to minimize the bit error rate (BER) between the original data at the transmitter and the finally decoded data at the receiver. While conventional communication systems require pilot signals to be transmitted separately from data for channel estimation, the proposed method enables communication without such pilot signals by allowing the AI models at both the transmitter and receiver to jointly learn the communication scheme. In the considered scenario, this leads to the adoption of an asymmetric constellation shape, which the receiver then learns to utilize for detecting the data without any pilot signals. This improves throughput by utilizing all the available resources for data transmission.

III. Experimental Environments

The training of the AI models was conducted offline using one million slots of simulated data, randomly generated within the parameter ranges specified in Table I. During training, Tapped Delay Line (TDL)-A, TDL-B, and TDL-C channel models defined in 3GPP TR 38.901 [11] were utilized to represent diverse radio propagation environments. After training, the receiver AI model was deployed on a GPU server for real-time inference. The inference was performed on real hardware and radio frequency (RF) channels. Note that there is no additional inference in the transmitter since it simply uses pre-learned constellations.

TABLE I. Parameter Configuration For The Training

Parameter	Configuration
Channel model	3GPP TDL-A, TDL-B, TDL-C
Velocity	0~200 km/h
Delay spread	10~500 ns
SNR	0~20 dB

A proof-of-concept (PoC) system was developed to evaluate the proposed method, the architecture of which is illustrated in Fig. 2. As mentioned above, baseband signal processing was performed on a GPU server, while a USRP X310 software-defined radio (SDR) platform was employed for signal transmission and reception. The transmitted signal from the USRP was delivered to the receiver either directly through a channel emulator or via an actual omnidirectional antenna, depending on the experimental configuration. In the case of over-the-air (OTA) testing, an amplifier was connected to the output of the USRP in order to ensure sufficient transmit power.

Table II summarizes the parameter settings of the PoC system. For the experimental evaluation, the 256 Quadrature Amplitude Modulation (QAM) Modulation and Coding Scheme (MCS) table defined in 3GPP was employed [12]. The selected MCS indices, ranging from 5 to 10, correspond to 16QAM modulation. In this experiment, the proposed AI-based pilotless communication method is compared with a conventional demodulation reference signal (DM-RS)-based method in 5G NR system, where DM-RSs are transmitted in 2 or 3 OFDM symbols per slot, depending on the tested

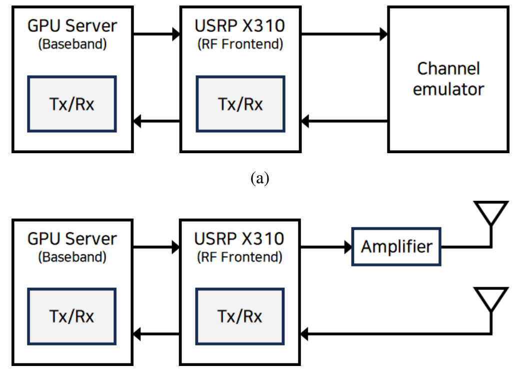

Fig. 2. PoC system architecture for (a) channel emulator-based testing and (b) over-the-air testing.

channel condition. In contrast, the proposed method does not transmit DM-RS, as there is no explicit channel estimation process. In both methods, the first OFDM symbol of each slot is reserved and not used for data transmission. Therefore, the proposed method utilizes 13 OFDM symbols per slot for data transmission, while the conventional method uses 10 or 11 OFDM symbols depending on the DM-RS configuration.

TABLE II. Parameter Configuration For The PoC System

Parameter	Configuration
Frequency band	3.7 GHz, 4.6 GHz
Bandwidth	9 MHz
Subcarrier spacing	30 kHz
Num. of subcarriers	300
MCS index	5~10 (16QAM)
Num. of DM-RS	2~3 symbols

For the channel emulator-based testing, TDL-A, TDL-B, and TDL-C channel models were created with representative velocity and delay spread values, as shown in Table III. For simplicity, each channel was assigned a numeric identifier, and the channel numbers are referenced hereinafter. Note that Channels 1 to 3 correspond to conditions within the training range, whereas Channel 4 represents a condition outside the training range.

TABLE III. Channel Models Adopted For Channel Emulator-Based Testing

Number	Channel model	Parameter configuration
1	TDL-A	UE velocity: 3km/h Delay spread: 30ns
2	TDL-B	UE velocity: 60km/h Delay spread: 100ns
3	TDL-C	UE velocity: 120km/h Delay spread: 300ns
4	TDL-C	UE velocity: 300km/h Delay spread: 300ns

IV. Experimental Results

In this section, we present the experimental results for the proposed method using the PoC system described in Section III. The tests are classified into two categories: channel emulator-based tests to emulate various channel conditions, and OTA tests to evaluate whether it performs well in real environments.

A. *Channel emulator-based test*

Fig. 3 shows the block-error-rate (BLER) performances of the proposed method over the emulated channels in the 3.7 GHz and 4.6 GHz bands. The MCS index was set to 7 for all the tests. For the DM-RS configuration, 2 symbols at the 4th and 10th positions in each slot were used for Channel 1 and Channel 2, while 3 symbols at the 2nd, 6th, and 10th positions in each slot were used for Channel 3 and Channel 4. Experimental results demonstrate that, under relatively favorable channel conditions such as Channel 1, the proposed method achieves BLER performance comparable to that of the conventional method. However, under scenarios where the channel conditions change rapidly, the results show that the conventional method, which performs channel estimation using DM-RS, suffers significant degradation in BLER performance. In contrast, it is observed that the proposed method, which is trained in a data-driven manner, maintains consistently good BLER performance across various channel conditions. Moreover, the proposed method continues to achieve good BLER performance on Channel 4, which is outside the range of the training environments, indicating that the proposed method can remain robust even in channel conditions that deviate from those seen during training.

Fig. 4 illustrates the effective throughput performance at the MCS index corresponding to a target BLER of 10^{-1}, evaluated with respect to channel signal-to-noise ratio (SNR). The transport block size (TBS) is calculated based on the time-frequency resources allocated within a single slot duration, as shown in equation (1), where N_{SC}, N_{Dsym}, M, and R denote the number of subcarriers, the number of PUSCH symbols per slot, the modulation order, and the code rate, respectively. Consequently, effective throughput is computed according to equation (2), where T_{slot} represents the slot duration.

$$TBS = N_{SC} \cdot N_{Dsym} \cdot M \cdot R \tag{1}$$

$$Effective\ throughput = (1 - BLER) \cdot TBS\ /\ T_{slot} \tag{2}$$

The equations imply that, when both the proposed method and the conventional method are configured with the same MCS index (M, R) and achieve identical BLER, the proposed method achieves a throughput gain of approximately 18.2% or 30%, depending on the ratio of the numbers of PUSCH symbols per slot between the two methods. For all tested conditions, the proposed method achieves a throughput gain of more than 15% compared to the conventional method. Furthermore, in rapidly varying channel conditions, the conventional method suffers from degraded BLER performance, thereby requiring the use of a lower MCS index compared to the proposed method at the same SNR. In the case of Channel 4, the conventional method fails to achieve the target BLER of 10^{-1} even with the MCS index of 5, the lowest available index in the PoC

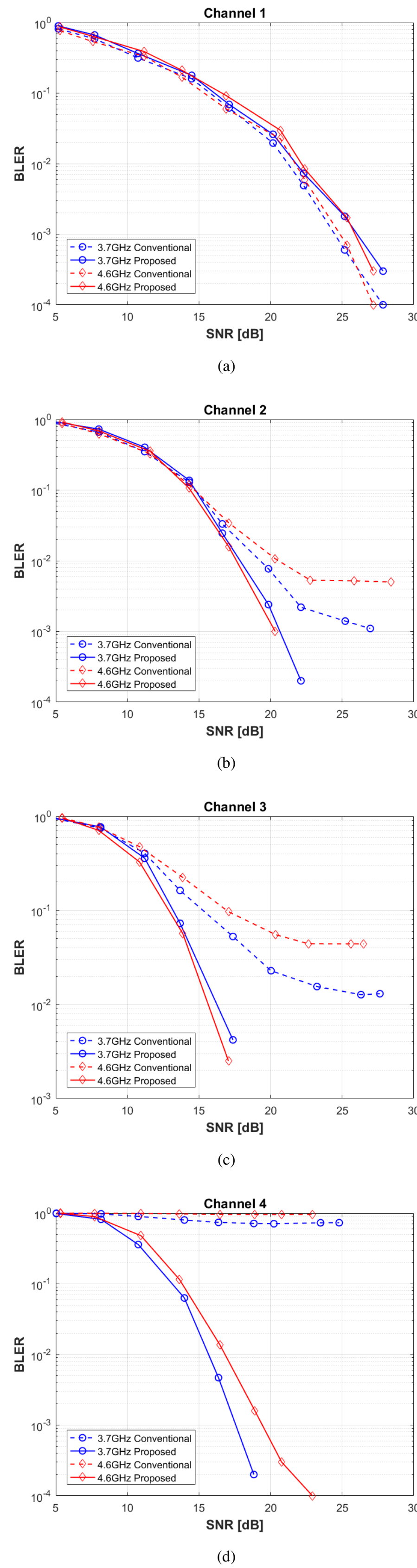

Fig. 3. BLER performance on
(a) Channel 1, (b) Channel 2, (c) Channel 3, and (d) Channel 4

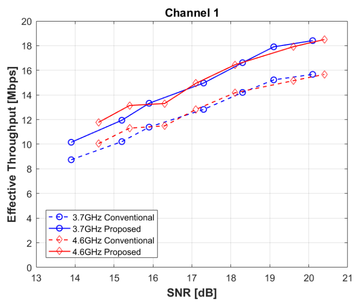

3.7GHz			4.6GHz		
SNR [dB]	MCS		SNR [dB]	MCS	
	Conv.	Prop.		Conv.	Prop.
13.9	5	5	14.6	6	6
15.2	6	6	15.4	7	7
15.9	7	7	16.3	7	7
17.3	8	8	17.1	8	8
18.3	9	9	18.1	9	9
19.1	10	10	19.6	10	10
20.1	10	10	20.4	10	10

(a)

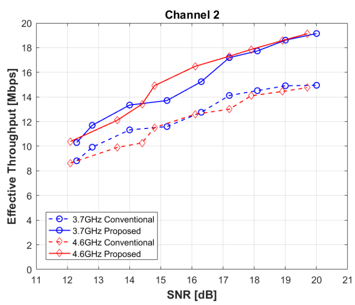

3.7GHz			4.6GHz		
SNR [dB]	MCS		SNR [dB]	MCS	
	Conv.	Prop.		Conv.	Prop.
12.3	5	5	12.1	5	5
12.8	6	6	13.6	6	6
14.0	7	7	14.4	6	7
15.2	7	7	14.8	7	8
16.3	8	8	16.1	8	9
17.2	9	9	17.2	8	9
18.1	9	9	17.9	9	10
19.0	9	10	18.9	9	10
20.0	10	10	19.7	9	10

(b)

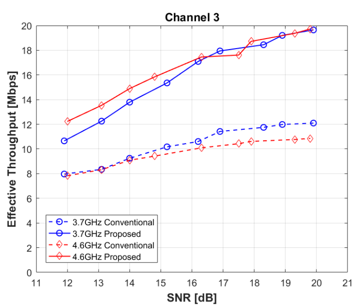

3.7GHz			4.6GHz		
SNR [dB]	MCS		SNR [dB]	MCS	
	Conv.	Prop.		Conv.	Prop.
11.9	5	5	12.0	5	6
13.1	5	6	13.1	5	7
14.0	6	7	14.0	6	8
15.2	7	8	14.8	6	8
16.2	7	9	16.3	7	9
16.9	8	9	17.5	7	10
18.3	8	10	17.9	7	10
18.9	8	10	19.3	7	10
19.9	8	10	19.8	7	10

(c)

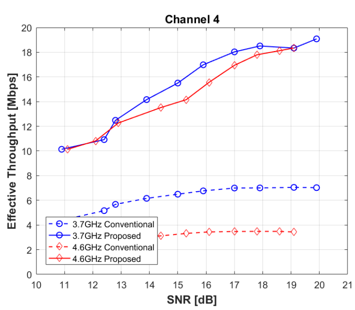

3.7GHz			4.6GHz		
SNR [dB]	MCS		SNR [dB]	MCS	
	Conv.	Prop.		Conv.	Prop.
10.9	5	5	11.1	5	5
12.4	5	5	12.1	5	5
12.8	5	6	12.9	5	6
13.9	5	7	14.4	5	7
15.0	5	8	15.3	5	7
15.9	5	9	16.1	5	8
17.0	5	9	17.0	5	9
17.9	5	9	17.8	5	9
19.1	5	10	18.6	5	9
19.9	5	10	19.1	5	9

(d)

Fig. 4. Effective throughput performance at the MCS index corresponding to a target BLER of 10^{-1} on (a) Channel 1, (b) Channel 2, (c) Channel 3, and (d) Channel 4

system, across all tested SNRs. As a result, the throughput gain achieved by the proposed method over the conventional method increases as the channel conditions become more dynamic.

B. Indoor over-the-air test

OTA tests were also conducted using physical antennas at SK Telecom's Bundang office. The tests were categorized into fixed-point and mobile tests, and Fig. 5 illustrates the photographs of the office environments and the test scenarios for both fixed-point and mobile tests. The receiving antenna was installed at the center of the office, whereas the transmitting antenna was either repositioned or moved at walking speed during the test. For all test scenarios, the MCS index was set to 10, and 2 symbols were used for DM-RS transmission in the conventional method.

Table IV and Table V summarize the test results of the proposed method and conventional method in the 3.7GHz and 4.6GHz band, respectively. In the fixed-point test, both the proposed and conventional methods exhibited almost no block errors. Consequently, the proposed method achieved approximately 18% throughput gains for all tested Tx points. In the mobile test, the proposed method improved the throughput performance by approximately 13–18% in the actual indoor environments.

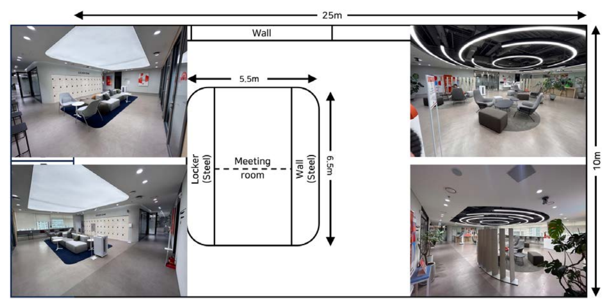

(a)

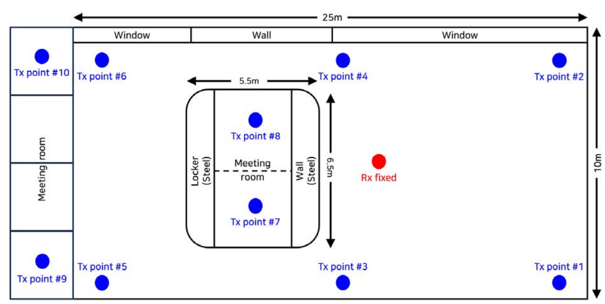

(b)

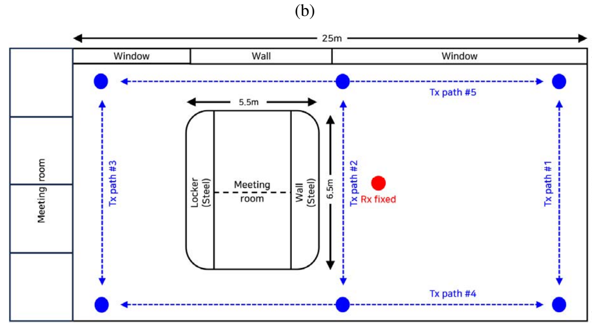

(c)

Fig. 5. Over-the-air test environments and scenarios. (a) photographs of the office environments, (b) fixed-point test scenarios, and (b) mobile test scenarios.

TABLE IV. INDOOR OVER-THE-AIR TEST RESULTS IN 3.7GHZ BAND

Fixed-point test							**Mobile test**						
Tx point	**SNR [dB]**	**BLER**		**Eff. T-put [Mbps]**		**T-put gain [%]**	**Tx path**	**SNR [dB]**	**BLER**		**Eff. T-put [Mbps]**		**T-put gain [%]**
		Conv.	**Prop.**	**Conv.**	**Prop.**				**Conv.**	**Prop.**	**Conv.**	**Prop.**	
#1	17.2	0.0000	0.0000	16.96	20.05	18.2	#1	18.6	0.0142	0.0125	16.72	19.80	18.4
#2	18.9	0.0000	0.0000	16.96	20.05	18.2	#2	22.5	0.0002	0.0001	16.96	20.05	18.2
#3	18.5	0.0000	0.0000	16.96	20.05	18.2	#3	17.8	0.0203	0.0318	16.62	19.41	16.8
#4	23.3	0.0000	0.0000	16.96	20.05	18.2	#4	21.5	0.0585	0.0620	15.97	18.81	17.7
#5	16.6	0.0000	0.0000	16.96	20.05	18.2	#5	23.0	0.0223	0.0335	16.59	19.38	16.8
#6	14.2	0.0000	0.0000	16.96	20.05	18.2	N/A						
#7	14.3	0.0000	0.0000	16.96	20.05	18.2							
#8	13.8	0.0000	0.0000	16.96	20.05	18.2							
#9	14.6	0.0000	0.0000	16.96	20.05	18.2							
#10	15.5	0.0000	0.0000	16.96	20.05	18.2							

TABLE V. INDOOR OVER-THE-AIR TEST RESULTS IN 4.6GHZ BAND

Fixed-point test							**Mobile test**						
Tx point	**SNR [dB]**	**BLER**		**Eff. T-put [Mbps]**		**T-put gain [%]**	**Tx path**	**SNR [dB]**	**BLER**		**Eff. T-put [Mbps]**		**T-put gain [%]**
		Conv.	**Prop.**	**Conv.**	**Prop.**				**Conv.**	**Prop.**	**Conv.**	**Prop.**	
#1	14.1	0.0000	0.0004	16.96	20.04	18.1	#1	22.3	0.0217	0.0237	16.60	19.57	17.9
#2	23.6	0.0000	0.0000	16.96	20.05	18.2	#2	22.4	0.0151	0.0270	16.71	19.51	16.8
#3	16.6	0.0009	0.0033	16.95	19.98	17.9	#3	19.4	0.0687	0.1076	15.80	17.89	13.2
#4	13.6	0.0000	0.0000	16.96	20.05	18.2	#4	19.6	0.0572	0.0638	15.99	18.77	17.4
#5	17.2	0.0000	0.0000	16.96	20.05	18.2	#5	20.1	0.0567	0.0904	16.00	18.24	14.0
#6	13.6	0.0000	0.0000	16.96	20.05	18.2	N/A						
#7	17.2	0.0000	0.0000	16.96	20.05	18.2							
#8	17.7	0.0000	0.0000	16.96	20.05	18.2							
#9	14.7	0.0000	0.0000	16.96	20.05	18.2							
#10	11.8	0.0000	0.0023	16.96	20.00	17.9							

V. CONCLUSION

In this paper, a PoC system for the AI-based pilotless communication method was developed and experimentally evaluated through channel emulation and OTA testing in practical indoor environments. The proposed method eliminates the need for pilot signals by using jointly trained AI models at both the transmitter and receiver, thereby enabling more efficient utilization of time-frequency resources.

Experimental results demonstrate that the proposed method consistently achieves higher throughput compared to the conventional 5G NR-based communication method, with robust BLER performance even under rapidly varying channel conditions and in environments not considered during training. OTA tests in real indoor settings further confirm the practical effectiveness of the proposed method, demonstrating a throughput gain of 13–18% over the baseline.

For future works, we plan to develop an AI model using real-world network data and evaluate its performance against the current simulation-trained model. In addition, we will upgrade the PoC system and conduct extensive field tests in outdoor and high-mobility environments to further validate the effectiveness and robustness of the proposed method.

REFERENCES

[1] NVIDIA, "Cosmos World Foundation Model Platform for Physical AI," Jan. 2025. [Online]. Available: https://arxiv.org/abs/2501.03575

[2] *Framework and overall objectives of the future development of IMT for 2030 and beyond*, recommendation ITU-R M.2160-0, ITU, Nov. 2023.

[3] H. Lee, K. Kim, G. Cho, G. Choi, S. Lee, M. Na, and T. Yu, "The Evolution Path of Telco Infrastructure: From Open RAN to 6G AI-RAN (Telco Edge AI)," *2024 15th International Conference on Information and Communication Technology Convergence (ICTC)*, Oct. 2024.

[4] GSMA and Kearney, "Mobile Infrastructure Investment Landscape," Mar. 2025. [Online]. Available: https://www.gsma.com/solutions-and-impact/connectivity-for-good/public-policy/gsma_resources/mobile-infrastructure-investment-landscape/

[5] J. Hoydis, F. A. Aoudia, A. Valcarce, and H. Viswanathan, "Toward a 6G AI-Native Air Interface," *IEEE Communications Magazine*, vol. 59, no. 5, pp. 76-81, May 2021.

[6] *New WID on Artificial Intelligence (AI)/Machine Learning (ML) for NR Air Interface*, document RP-234039, 3GPP, Dec. 2023.

[7] J. Pihlajasalo, D. Korpi, M. Honkala, J. M. J. Huttunen, T. Riihonen, J. Talvitie, A. Brihuega, M. A. Uusitalo, and M. Valkama, "Deep Learning OFDM Receivers for Improved Power Efficiency and Coverage," *IEEE Transactions on Wireless Communications*, vol. 22, no. 8, pp. 5518-5535, Aug. 2023.

[8] J. M. J. Huttunen, D. Korpi, and M. Honkala, "DeepTx: Deep Learning Beamforming With Channel Prediction," *IEEE Transactions on Wireless Communications*, vol. 22, no. 3, pp. 1855-1867, Mar. 2023.

[9] M. Honkala, D. Korpi, and J. M. J. Huttunen, "DeepRx: Fully Convolutional Deep Learning Receiver," *IEEE Transactions on Wireless Communications*, vol. 20, no. 6, pp. 3925-3940, Jun. 2021.

[10] F. A. Aoudia and J. Hoydis, "End-to-End Learning for OFDM: From Neural Receivers to Pilotless Communication," *IEEE Transactions on Wireless Communications*, vol. 21, no. 2, pp. 1049-1063, Feb. 2022.

[11] *Study on channel model for frequencies from 0.5 to 100 GHz*, document TR38.901 V18.0.0, 3GPP, Mar. 2024.

[12] *NR; Physical layer procedures for data*, document TS 38.214 V18.5.0, 3GPP, Jan. 2025.